end-to-end distance of the reacting radical, $\langle l^2 \rangle^{1/2}$. Comparing calculated and experimental results, one finds that the only serious deviation is where one would expect to find it, namely with the octadecyl radical. The remaining rate constants show agreement within experimental error. There are two points, concerning these results which must be discussed.

First, one notices that the deviation between theory and experiment for the octadecyl radical may be an indication that such long-chain species do not react at every encounter. An alternative interpretation is that an encounter between long-chain species involves a certain amount of interpenetration before reaction can occur so that the effective encounter diameter is actually less than $\langle l^2 \rangle^{1/2}$. The present experiments are not able to provide a distinction between these two interpretations.

The second notable point concerning the data of Table III has to do with the results for the pentyl radical. The value of k_t for this radical is unusually small, but so is its measured diffusion coefficient; hence, one finds good agreement between experimental and calculated values of k_t. Since both k_t and D are determined by making rate measurements on the same monitor reaction, it was decided to review this reaction to try to determine whether or not it contained a source of error for these measurements. Since the results for the other three radicals seemed to be in reasonable accord with expectations, and since triethyl phosphite is a reagent common to all of the reactions, one tries to find a singularity associated with the thiol or with the corresponding thiyl or alkyl radical. It appears that the most likely point at which one of these species could be trapped so that translational motion might be inhibited would be in connection with eq 3. Here the pentyl radical may exist as a caged pair with $SP(OEt)_3$ and undergo a number of nonrandom diffusive displacements before moving into the bulk solution. Presumably, propyl radicals are small enough to enjoy more efficient escape and dodecyl and octadecyl are large enough so that only a small fraction of the chain molecule is ever trapped. Thus, the results of these studies, while useful in interpreting the diffusion-controlled nature of k_t for some radicals, may not be as generally applicable as one would like. These results also indicate the need for devising systems in which radicals are produced in a kinetically free state if solution properties of these reactive species are to be studied.

Acknowledgments. This work was supported by the U. S. Atomic Energy Commission under Contract No. AT(04-3)727 and by the donors of the Petroleum Research Fund, administered by the American Chemical Society. Assistance with some of the experimental work by Vincent H. Knauf II is acknowledged.

On the Flexibility of Hydrocarbon Chains in Lipid Bilayers[1]

Joachim Seelig

Contribution from the Physikalisch-Chemisches Institut der Universität Basel, CH-4056 Basel, Switzerland. *Received October 22, 1970*

Abstract: The spin label technique is used to investigate the flexibility of the hydrocarbon chains of a smectic phase with bilayer structure. The experimental data, especially the temperature dependence of the flexibility, can be explained in terms of a phenomenological theory which is based on the mathematical formalism of the rotational isomeric model. This approach leads to conclusions about the apparent configurational entropy per methylene group which are consistent with calorimetric data.

Bilayer structures play an important role in biological membranes, and detailed knowledge of the way bilayer lipids are organized will eventually lead to an understanding of membrane properties.[2,3] One intriguing aspect of the rather complex situation is the configuration of the hydrocarbon chains in the lipid bilayer. In a previous publication we have shown how the spin label technique can be employed in solving this question.[4] Briefly, our investigation of smectic liquid crystals and phospholipid dispersions has resulted in the following findings. (1) The lipid bilayers are highly fluid in the sense that the hydrocarbon chains are rotating rapidly ($>10^8$ cps) around their long molecular axes. (2) The hydrocarbon chains are neither coiled nor completely extended; instead, the experiments reveal a high degree of order of the hydrocarbon chain in the region adjacent to the hydrophilic environment, which decays exponentially when going into the hydrophobic interior. This decrease of the degree of order is due to the intrinsic flexibility of the hydrocarbon chains. We have now extended our earlier measurements to determine the temperature dependence of this flexibility. Furthermore, we wish to describe how the experimental data can be explained to a first approximation, by applying a phenomenological theory using the formalism of the rotational isomeric model.[5-7] This approach will also enable us to calculate the apparent configurational entropy per

(1) Work supported by the Swiss National Foundation under Grant No. 3,131,69.

(2) W. Stoeckenius and D. M. Engelman, *J. Cell Biol.*, **42**, 613 (1969).

(3) D. Chapman, Ed., "Biological Membranes," Academic Press, London, 1968.

(4) J. Seelig, *J. Amer. Chem. Soc.*, **92**, 3881 (1970).

(5) M. V. Volkenstein, "Configurational Statistics of Polymeric Chains," Interscience, New York, N. Y., 1963.

(6) T. M. Birshtein and O. B. Ptitsyn, "Conformations of Macromolecules," Interscience, New York, N. Y., 1966.

(7) P. J. Flory, "Statistical Mechanics of Chain Molecules," Interscience, New York, N. Y., 1969.

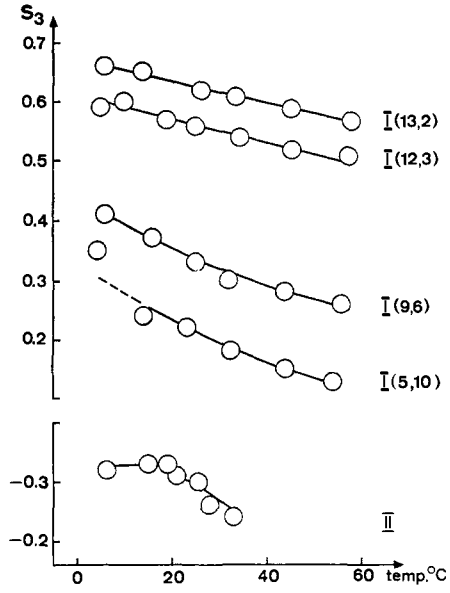

Figure 1. Temperature dependence of the degree of order S_3 for the spin labels of series I and II.

methylene group which can then be compared with pertinent calorimetric data. We restrict our investigation to completely saturated hydrocarbon chains of the polyethylene type.

Materials and Experimental Results

The experimental conditions are almost identical with those described previously. The liquid crystalline model system consists of sodium decanoate (~28 wt %), *n*-decyl alcohol (~42 wt %), and water (~30 wt %). This mixture forms well-defined bilayers[8] which can be oriented homogeneously in a rectangular esr sample cell with closely spaced surfaces. In order to use the Varian temperature-control equipment E-9540 it was necessary to construct a rectangular sample cell with the dimensions 45 × 4 × 0.05 mm. This cell is slightly smaller than the one used in our earlier work, but the orienting effect with regard to the lipid bilayers is virtually unchanged. The temperature in the middle of the cavity was measured immediately before and after each esr experiment and was found to remain constant within ±0.5°. Nevertheless, the reported temperatures are only average values, since the temperatures at the upper and the lower edges of the cavity differ by approximately 2°.

As spin labels we have used stearic acid derivatives of type I(*m*, *n*) and the steroid nitroxide II. Details of the chemical synthesis and physical characteristics may be found in ref 4 and 9. One essential difference between labels I and II is the complete rigidity of the steroid frame compared to the rather flexible fatty acid backbone.

The experimentally accessible quantity is the orientation of the nitroxide group with respect to the optical axis of the oriented liquid crystalline system, as determined by the degree of order S_3 (*cf.* ref 4). Since the spin label group is rigidly bound to the carbon skeleton of the fatty acid and the steroid molecule, the

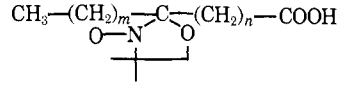

I(*m*,*n*)
I(13,2); I(9,6)
I(12,3); I(5,10)

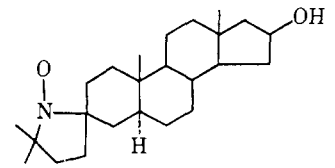

II

quantity S_3 therefore yields information about the orientation of the whole molecule.

Figure 1 shows the temperature dependence of the degree of order S_3 for the various fatty acids and the steroid spin label. The experimental points were obtained by the following procedure. The bilayer phase was doped with spin label and oriented homogeneously in the esr sample cell. The system was then placed in the esr cavity with the normal of the large glass surface pointing parallel and perpendicular, respectively, to the directions of the magnetic field. At each temperature spectra of both orientations were recorded. These spectra resemble those in Figure 1, ref 4. The quantitative evaluations followed along the lines set out in section II, ref 4. First, we have calculated the isotropic hyperfine splitting constant a, which was found to be temperature independent within the range of 5–50° for the fatty acid spin labels and 5–35° for the steroid spin label. Therefore, we have restricted our investigation to these temperature ranges. Next, we have determined T_{xx} and T_{zz}, the tensor components of the NO group in its specific molecular coordinate system, which were then used to calculate S_3. The actual numbers for a, T_{xx}, and T_{zz} are almost the same as those given in Table I and II of ref 4. There are some small deviations (~±0.2 G) which we attribute to a better temperature control and to a larger number of measurements, which have helped to reduce the statistical error.

Two comments on the upper and lower temperature boundaries of our experiments seem appropriate. (1) At ~40° the bilayer begins to melt and is found to be in equilibrium with a second phase. The esr spectrum clearly discloses two types of motion, an anisotropic rotation, due to spin labels incorporated in the bilayer phase, and a random tumbling, due to spin labels in an isotropic liquid. With increasing temperature the equilibrium is shifted toward the isotropic phase. Because of the superposition of two different spectra, an unambiguous quantitative interpretation becomes impossible at temperatures above 50°. The experiments with the steroid label II are subjected to this difficulty at an even lower temperature, since the spectral difference between the isotropic and anisotropic rotation is not so distinct in this case as it is for the labels of series I. (2) Below ~0° the transition from the liquid crystalline to the solid state occurs. The esr spectrum is still dependent on the orientation with respect to the magnetic field as can be seen from Figure 2, but it has more similarity to a powder spectrum than to an oriented single-crystal spectrum, even though the

(8) J. Seelig, manuscript in preparation.
(9) W. L. Hubbell and H. M. McConnell, *Proc. Nat. Acad. Sci. U. S.*, 63, 16 (1969).

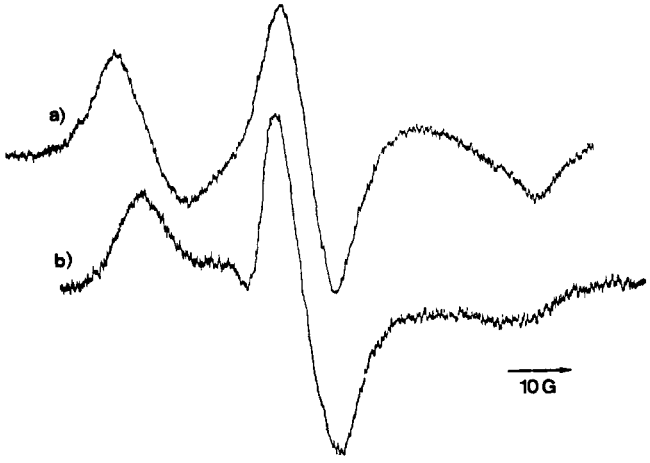

Figure 2. Spin label I (13, 2) in an oriented sample of smectic liquid crystals at −60°: (a) magnetic field parallel to the normal of the cell surface, (b) magnetic field perpendicular to the normal of the cell surface.

degree of order of this specific label amounts to $S_3 \sim 0.7$ in the liquid crystalline phase. We therefore conclude that during the process of crystallization a reordering of the lipid molecules takes place which destroys the homogeneous orientation of the bilayers.

Let us now return to the experimental results described in Figure 1. If we compare the spin labels of series I at one specific temperature, we observe a decrease in the degree of order S_3 if the label group is moved into the interior of the bilayer. This effect is caused by the intrinsic flexibility of the hydrocarbon chain, and we have already given a quantitative description using the worm-like model of Porod and Kratky.[10] We have obtained the following expression for the dependence of S_3 on the position of the spin label group[4]

$$\log S_3 = \text{constant} + k \log S_\alpha \qquad (1)$$

Here, k represents the number of carbon–carbon bonds between the polar group and the spin label group, whereas S_α is a measure of the intrinsic flexibility of the hydrocarbon chain. In Figure 3 the degree of order S_3 is plotted according to eq 1 for two different temperatures. (The actual points of Figure 3 are interpolated from Figure 1.) The slope of the resulting straight lines determines S_α. S_α is obviously temperature dependent, and Table I summarizes the corresponding numerical

Table I

Temp, °C	Slope	S_α	$\langle \cos^2 \alpha \rangle$
10	−0.057	0.876	0.918
20	−0.066	0.860	0.906
30	−0.074	0.843	0.896
40	−0.081	0.831	0.887
50	−0.086	0.821	0.881

results for several different temperatures. Since S_α is a semiempirical parameter which clearly defines the hydrocarbon chain flexibility, we must ask how this coefficient can be understood on a molecular basis.

(10) O. Kratky and G. Porod, *Recl. Trav. Chim. Pays-Bas*, **68**, 1106 (1949).

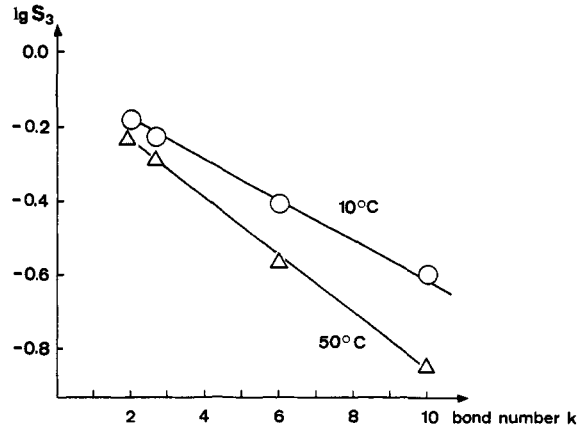

Figure 3. Dependence of S_3 on the bond number k for two different temperatures.

The Rotational Isomeric Model and the Flexibility of Hydrocarbon Chains

The rotational isomeric model of a polymeric chain closely resembles the molecular geometry and physical behavior of a real polymer. The two main features of this model are the following.[5-7] (1) The rotations of the bonds forming the polymer backbone are restricted to discrete angles of rotation. In the case of a polymer of the polyethylene type, the allowed conformations of the carbon–carbon bonds are the trans conformation (t) and two gauche conformations (g^+, g^-). These conformations correspond to minima in the potential energy of the system and are separated from each other by rather steep energy barriers. Nevertheless, these barriers are not high enough to prevent the bonds from jumping rapidly from one conformation to the other. This rotational isomerization (frequency $>10^{10}$ cps) leads to different configurations of the macromolecule and is the reason for the flexibility of the polymer. It should be pointed out that the three conformations do not have the same energy but that the trans form is normally more stable by a few hundred calories per mole. (2) The conformational rotations are not independent of each other; instead, the model assumes a first-neighbor interaction. All statistical calculations describing the properties of the polymer are carried out by taking into account the linear cooperativity of the system.

A wealth of experimental evidence supporting this model has been accumulated by studies of polymer solutions, and it is tempting to apply a similar approach to the hydrocarbon chains of a liquid crystalline bilayer. The essential difference between the two situations is due to the intermolecular interactions which, in the case of the liquid crystalline phase, are forcing the molecules into the bilayer arrangement, but which are completely negligible for diluted isotropic solutions. An exact theory for the treatment of intermolecular interactions in a bilayer has not yet been developed and is not attempted in the present investigation. Instead, the following approximation is introduced to provide a preliminary quantitative explanation of the experimental data. The hydrocarbon chains are treated as if their increased stiffness in the bilayer is due to an apparent increase in the energy difference E_σ between the trans and gauche conformations; *i.e.*, E_σ is no

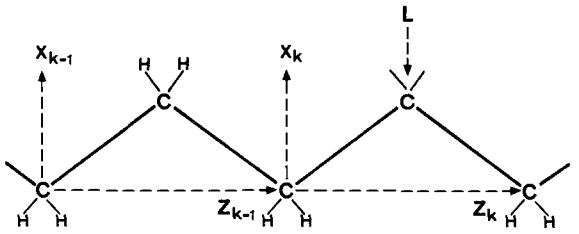

Figure 4.

longer regarded as a pure intramolecular rotational potential but as an empirical factor which comprises contributions from intra- as well as intermolecular forces. Obviously, this assumption leads to a phenomenological theory. (The approach can be compared, in essence, with the assumption of a reaction field in dipole theory or that of a *macroscopic* viscosity in molecular diffusion theory.) Using the mathematical formalism of the normal rotational isomeric model, this empirical approach leads to two improvements compared to the Porod–Kratky model. First, it takes into account a rapid, cooperative rotational isomerization of the carbon–carbon bonds. Secondly, all experimental facts can be accommodated in a model which contains just one free parameter. Clearly, this model must fail if the properties of the bilayer closely resemble that of a crystalline phase. Fortunately, the large motional freedom of the spin labels enables the assumption to be made that the bilayer of our special system is highly fluid and, therefore, more closely resembles a liquid phase than a crystalline phase.

Using Flory's notation,[7] we can now proceed to derive quantitative expressions for the flexibility of the hydrocarbon chains in the bilayer. Let us consider a polyethylene chain of n carbon–carbon bonds. Each bond, except the two terminal ones, can occur in three conformations designated t, g^+, and g^-. The apparent energy difference between the trans state and the gauche states is denoted by E_σ, which leads to a statistical weight factor for the gauche states of

$$\sigma = \exp(-E_\sigma/RT) \tag{2}$$

if the statistical weight of the trans form is arbitrarily defined as 1. In order to evaluate the configurational partition function Z we introduce a statistical weight matrix $\mathbf{U}$.

$$\begin{array}{c} \\ \mathrm{t} \\ \mathrm{g}^+ \\ \mathrm{g}^- \end{array} \begin{array}{c} \begin{array}{ccc} \mathrm{t} & \mathrm{g}^+ & \mathrm{g}^- \end{array} \\ \begin{bmatrix} 1 & \sigma & \sigma \\ 1 & \sigma & 0 \\ 1 & 0 & \sigma \end{bmatrix} \end{array} = \mathbf{U} = [u_{\xi\eta}] \tag{3}$$

(The conformations g^+g^- and g^-g^+ are excluded as unrealistic from our model.) The configurational partition function Z is then found to be

$$Z = [1\ 0\ 0]\mathbf{U}^{n-2}\begin{bmatrix}1\\1\\1\end{bmatrix} \tag{4}$$

The purpose of this matrix formalism is to take into account the cooperativity of the system. Diagonalization of Z simplifies the calculation

$$Z = [1\ 0\ 0]\mathbf{A}\mathbf{\Lambda}^{n-2}\mathbf{B}\begin{bmatrix}1\\1\\1\end{bmatrix} \tag{5}$$

where

$$\mathbf{B} = \mathbf{A}^{-1} \tag{6}$$

and

$$\mathbf{BUA} = \mathbf{\Lambda} \tag{7}$$

$\mathbf{\Lambda}$ is the diagonal matrix of the eigenvalues of $\mathbf{U}$.

$$\mathbf{\Lambda} = \begin{bmatrix}\lambda_1 & 0 & 0\\ 0 & \lambda_2 & 0\\ 0 & 0 & \lambda_3\end{bmatrix} \tag{8}$$

For long chains, the partition function Z is determined by the largest eigenvalue of $\mathbf{U}$.

$$Z = \lambda_1^{n-2} \qquad n \to \infty \tag{9}$$

Let us introduce two further matrices. The first contains the *a priori* probabilities of a given bond pair.

$$\mathbf{P} = [p_{\xi\eta}] \tag{10}$$

E.g., p_{g^+t} means the probability of finding two neighboring bonds in g^+ and t conformations, respectively. For long chains these probabilities can be calculated by the following expression.

$$p_{\xi\eta} = u_{\xi\eta}A_{\eta 1}B_{1\xi}/\lambda_1 \qquad n \to \infty \tag{11}$$

The second matrix contains the conditional probabilities

$$\mathbf{Q} = [q_{\xi\eta}] \tag{12}$$

The elements of $\mathbf{Q}$ are given by

$$q_{\xi\eta} = u_{\xi\eta}A_{\eta 1}/A_{\xi 1}\lambda_1 \qquad n \to \infty \tag{13}$$

Equations 11 and 13 together enable us to calculate *a priori* probabilities of higher order, *e.g.*

$$p_{\epsilon\xi\eta} = p_{\epsilon\xi}q_{\xi\eta} \qquad n \to \infty \tag{14}$$

Let us now proceed to establish the relationship between the orientation of the spin label group and the orientation of the hydrocarbon chain. To this purpose we divide the polymeric chain into monomer units containing two bonds each. To each monomer unit—numerated serially..., $k-1$, k, $k+1$, ...—we attribute a Cartesian coordinate system X_k, Y_k, Z_k. The direction of the X_k and Z_k axes is indicated in Figure 4; the direction of the Y_k axis is arbitrary but identical for all monomer units. If the spin label group is attached in the middle of a monomer unit (position L in Figure 4) it is found, either by inspection of Corey–Pauling–Koltun models or by appropriate mathematical transformations, that the nitrogen $2p\pi$ orbital is extended exactly parallel to the corresponding Z_k axis. The degree of order S_3 as determined by the esr experiment is therefore identical with the orientation of the Z_k axis of the monomer unit to which the label is bound. We may thus confine our analysis of the flexibility to an investigation of the correlation of the Z_k axes with respect to each other. If we designate β as the angle between the Z_{k-1} axis and the Z_k axis, we may ask how β depends on the various conformations which the kth monomer unit can assume. A general solution to

this problem, describing the complete matrix for a transformation of the kth coordinate system into the $(k-1)$ one, is found in ref 6, p 158. Assuming tetrahedral valence angles for all carbon–carbon bonds, these formulas lead to the following results. (1) If both bonds of the kth monomer unit are in the trans conformation (tt), Z_k has the same direction as Z_{k-1}, *i.e.*, $\beta = 0°$ ($\cos^2\beta = 1$). (2) In the case of tg^+, tg^-, g^+t, or g^-t conformations, the two axes make an angle of $\beta = 60°$ ($\cos^2\beta = 1/4$) with each other. (3) In the conformations g^+g^+ and g^-g^-, Z_k and Z_{k-1} are at right angles to each other; $\beta = 90°$ ($\cos^2\beta = 0$). These results can also be verified by inspection of models. In order to obtain the average deviation of the Z_k axis from the Z_{k-1} axis, we multiply each $\cos^2\beta$ by the *a priori* probability of the corresponding configuration and sum.

$$\langle\cos^2\beta\rangle = p_{tt} + p_{tg} \tag{15}$$

In deriving eq 15, we have made use of the relation

$$p_{tg^+} = p_{tg^-} = p_{g^+t} = p_{g^-t} \tag{16}$$

Using eq 15, we can also calculate the degree of order S_β, which is defined as

$$S_\beta = (1/2)(3\langle\cos^2\beta\rangle - 1) \tag{17}$$

Equation 17 is our final expression for the flexibility between two monomer units. It should be remembered that this flexibility is caused by the rotational isomerization of the *two* carbon–carbon bonds in the kth monomer unit. Therefore, S_β should be equal to the square of S_α, *i.e.*, the flexibility of *one* bond expressed in terms of the Porod–Kratky model.

The proof for the latter contention may be shown by the fact that the correlation between monomer units, as expressed in terms of the rotational isomeric approach, is decreasing exponentially the more the two units are separate from each other. Let us therefore evaluate the mean deviation between the Z_k and the Z_{k-2} axes. The flexibility is now determined by the rotational isomerization of four carbon–carbon bonds, and we must take into account a total of 41 allowed configurations. Using eq 11, 12, and 14 we can calculate the *a priori* probability of each configuration. By means of appropriate transformation matrices, we also obtain the corresponding angle γ between the Z_k and the Z_{k-2} axis. After averaging, the final result reads

$$\begin{aligned}\langle\cos^2\gamma\rangle = {} & p_{tt}[q_{tt}^2 + (1/2)q_{tt}q_{tg^+} + \\ & (1/2)q_{tg^+}q_{g^+t}] + p_{tg^+}[(1/2)q_{tt}^2 + (1/2)q_{tt}(q_{tg^+} + \\ & q_{g^+t}) + 5q_{g^+t}q_{tg^+} + q_{tg^+}q_{g^+g^+} + (1/2)q^2_{g^+g^+}] + \\ & p_{g^+g^+}[q_{g^+t}q_{tg^+} + (1/2)q_{g^+g^+}q_{g^+t} + 2q^2_{g^+g^+}]\end{aligned} \tag{18}$$

the flexibility S_γ is then defined by

$$S_\gamma = (1/2)(3\langle\cos^2\gamma\rangle - 1) \tag{19}$$

Comparing eq 15 and 18, it is obvious that S_γ in general is not equal to S_β^2, which is the assertion of the Porod–Kratky model. However, it turns out that in our specific experimental situation the numerical difference between S_γ and S_β^2 is so small that the approximation $S_\gamma \approx S_\beta^2$ is completely justified. We may therefore write

$$S_\gamma^{1/2} \approx S_\beta \approx S_\alpha^2 \tag{20}$$

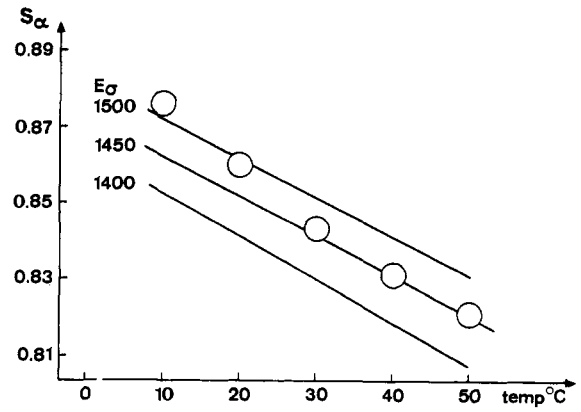

Figure 5. Temperature dependence of S_α. Experimental and theoretical results.

or

$$S_\beta^{1/2} \approx S_\alpha \tag{21}$$

We have thus related our theoretical model (S_β) with the experimentally accessible quantity (S_α). Since S_β is determined unambiguously by (eq 2) the only two parameters of our model are the temperature and the energy difference between the trans and the gauche conformation. If we make a judicial guess of E_σ, we can then calculate S_β for different temperatures and compare this with the experimental results.

Discussion

Figure 5 summarizes the theoretical and experimental results of the temperature dependence of S_α. The solid lines correspond to $S_\alpha = S_\beta^{1/2}$ and have been calculated as described in the preceding section with E_σ = 1400, 1450, and 1500 cal/mol, respectively. Inspection of Figure 5 reveals that the predicted increase in the chain flexibility, *i.e.*, the decrease of S_α, is rather small and that according to the theory S_α should be a virtually linear function of the temperature in the temperature range under consideration. The experimental results are represented by the circles, and the best agreement between the experiment and the theoretical calculations is given by E_σ = 1450 cal/mol. Two comments are necessary. (1) The absolute values of S_α as determined experimentally may be wrong by as much as ± 0.01. The energy difference E_σ is therefore subject to an error of *ca.* ± 100 cal/mol. The assumption of infinitely long chains in our calculation is not too serious a restriction, since the cooperative interaction is not very strong. Nevertheless, this simplification together with the exclusion of g^+g^- and g^-g^+ conformations and the assumption of perfectly tetrahedral bond angles are sources of additional errors. Making allowance for these shortcomings of our model would entail a considerable increase of the computational effort without any essential change in the numerical results. (2) At lower temperatures the experimental points deviate from the straight line toward larger values of E_σ. This effect can be understood as a consequence of the increased intermolecular interactions at low temperatures, which reduce the probability of the gauche conformation and tend to stretch the hydrocarbon chains into a more extended configuration, thus preforming the crystalline state.

It should be noted at this point that the steroid label II shows no change in the degree of order S_3 over the range 5–20° (Figure 1), whereas all labels of series I in the same region indicate a tendency of the bilayer toward a more random structure. These seemingly contradictory observations can be reconciled by the fact that the steroid label II has no intrinsic flexibility, from which it follows that an increase of the temperature near the crystalline liquid-crystalline transition point leaves the positional orientation of the molecules practically unaltered but affects primarily the configurational order within the hydrocarbon chain.

The feature of most importance for our discussion is the energy difference E_σ between the trans and the gauche conformations, which, according to Figure 5, amounts to approximately 1500 cal/mol for the liquid-crystalline phase at 20°, while values of 500–800 cal/mol are reported for liquid *n*-alkanes.[6,7] The trans conformation is thus more probable in the liquid-crystalline phase than in the liquid phase, and the difference between the two energies is a quantitative measure of the greater order or disorder prevailing in the two phases. Using the above numbers, we are in a position to calculate the configurational partition function, which gives complete information on the configurational structure and the thermodynamic functions of the hydrocarbon chains in the liquid-crystalline and the liquid situation. We are interested in the preference of the molecule to exhibit a trans conformation and we can calculate p_t according to eq 14. The results are $p_t = 0.88$ for the liquid-crystalline phase ($E_\sigma = 1500$ cal/mol, 20°) and $p_t = 0.65$ for the liquid phase ($E_\sigma = 500$ cal/mol, 20°). The difference between the two phases becomes more obvious if we calculate the probability of finding seven consecutive carbon–carbon bonds in the trans conformation. We obtain $p_{t7} = 0.40$ for the liquid crystal and $p_{t7} = 0.03$ for the isotropic liquid. A sequence of seven conformations is equivalent to a segment of nine carbon–carbon bonds, which in turn is the chain length of the molecules composing the bilayer (*e.g.*, *n*-decyl alcohol). We therefore conclude that the all-trans conformation is of considerable importance in the bilayer phase but negligible in the isotropic liquid.

We can also show that our contention $S_\gamma^{1/2} \approx S_\beta$ (eq 21) is approximately fullfilled for the liquid-crystalline phase. The calculation of S_β and $S_\gamma^{1/2}$ according to eq 15, 17, 18, and 19 with $E_\sigma = 1500$ cal/mol (20°) yields $S_\beta = 0.742$ and $S_\gamma^{1/2} = 0.740$. The exponential decrease of the degree of order S_3 as detected by the spin labels and as previously explained by the Porod–Kratky model is therefore equally well described by the more realistic rotational isomeric scheme. The corresponding numbers for the liquid phase are $E_\sigma = 500$ cal/mol, $S_\beta = 0.278$, and $S_\gamma^{1/2} = 0.255$. The small but distinct discrepancy between the latter values indicates that the correlation between two bonds decreases faster than exponentially in the case of very flexible chains.

The knowledge of the partition function Z also provides insight into the configurational entropy S of the polymeric chain. (S should not be confused with the degree of order as denoted by S_3, S_α, etc.) The standard expression for the entropy is given by

$$S = R \ln Z + RT(\partial \ln Z/\partial T) \qquad (22)$$

Using eq 9, we obtain the following approximation for the configurational entropy per hydrocarbon methylene group $s = S/n$

$$s = R \ln \lambda_1 + RT(\partial \ln \lambda_1/\partial T) \quad n \to \infty \qquad (23)$$

A list of λ_1's calculated with $E_\sigma = 1500$ cal/mol for a series of different temperatures is given in Table II. As

Table II

Temp, °C	$E_\sigma = 1500$ cal/mol λ_1	s, eu	$E_\sigma = 500$ cal/mol s, eu
10	1.131	0.82	1.57
20	1.141	0.86	1.61
30	1.154	0.90	1.65
40	1.166	0.94	1.69
50	1.178	0.98	1.72

a first tentative approximation, $\ln \lambda_1$ is a linear function of T, yielding a temperature coefficient of $(\partial \ln \lambda_1/\partial T) = 1.028 \times 10^{-3}$ °K^{-1}, which is used in eq 23 to calculate the configurational entropies s listed in the third column of Table II. Performing the same mathematical procedure with $E_\sigma = 500$ cal/mol leads to the configurational entropies of the liquid hydrocarbon chains (last column of Table II). Insofar as the approximations made in our model are adequate, the following conclusion can be drawn. The configurational entropy per hydrocarbon methylene group is only moderately temperature dependent, but the configurational disorder in the liquid phase, when expressed in terms of the entropy, is almost twice as large as that in the liquid-crystalline phase.

In order to find experimental evidence for this result we have resorted to a calorimetric study of liquid hydrocarbons and liquid crystalline bilayers by Phillips, *et al.*[11] The configurational entropies per methylene group as reported by these authors are in the range of 0.45–1.25 eu for the liquid-crystalline systems and 1.9–2.6 eu for the isotropic hydrocarbon liquids. Again it can be seen that the transition from the liquid-crystalline state to the liquid state increases the configurational entropy by roughly a factor of 2, thus lending support to our spin label results. The discrepancies in the numerical results are easily explained, since the calorimetric measurements were performed with systems differing in chemical composition from our smectic phase and also because the extrapolation procedure used by the authors leaves some ambiguity about the temperature to which the entropies refer.

In conclusion, we want to point out that our model is only a crude approximation to the real situation. The influence of intermolecular interactions is considered by using an empirical parameter. Nevertheless, this approach seems to be justified, since it yields a consistent explanation of all the experimental data and sheds some light on the physical state of a highly fluid bilayer.

Acknowledgment. The author wishes to thank Dr. W. Balthasar, Dr. B. H. Robinson, and Professor Dr. G. Schwarz for valuable comments.

(11) M. C. Phillips, R. M. Williams, and D. Chapman, *Chem. Phys. Lipids*, 3, 234 (1969).